Inorganic Chemistry

Article

pubs.acs.org/IC

Reticular Synthesis of a Series of HKUST-like MOFs with Carbon Dioxide Capture and Separation

Hongming He,[†,‡] Fuxing Sun,[†] Shengqian Ma,[*,‡] and Guangshan Zhu[*,†]

[†]State Key Laboratory of Inorganic Synthesis and Preparative Chemistry, College of Chemistry, Jilin University, Changchun 130012, China

[‡]Department of Chemistry, University of South Florida, 4202 East Fowler Avenue, Tampa, Florida 33620, United States

Supporting Information

ABSTRACT: We reported a series of HKUST-like MOFs based on multiple copper-containing secondary building units (SBUs). Compound **1** is constructed by two SBUs: $Cu_2(CO_2)_4$ paddle-wheel SBUs and Cu_2I_2 dimer SBUs. Compound **2** has $Cu_2(CO_2)_4$ paddle-wheel SBUs and Cu_4I_4 SBUs. Furthermore, compound **3** possesses $Cu_2(CO_2)_4$ paddle-wheel SBUs, Cu_2I_2 dimer SBUs, and $Cu(CO_2)_4$ SBUs. These compounds are promising materials for CO_2 capture and separation, because they all display commendable adsorption of CO_2 and high selectivity for CO_2 over CH_4 and N_2. It is worthy to note that compound **1** exhibits the highest Brunauer–Emmett–Teller surface area (ca. 901 $m^2\ g^{-1}$) among the MOF materials based on Cu_xI_y SBUs. In addition, compound **3** is the first case that three copper SBUs coexist in MOFs.

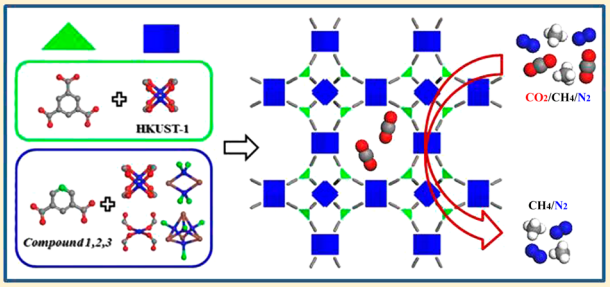

INTRODUCTION

Recently, metal–organic frameworks (MOFs),[1−4] as a prominent category of crystalline porous materials, have captivated considerable attention from chemists and materials scientists, not only because of their great potential applications in various research areas[5−13] but also by reason for their unparalleled designability through reticular synthesis.[14−22] MOFs can be successfully generated from organic bridging ligands and metal ions/clusters through coordination bonds. Extensive efforts have been devoted to building and constructing a desired structure by judiciously adjusting the suitable organic linkers and secondary building units (SBUs) to match the vertex of a given net. Nevertheless, some MOF platforms have been reported, e.g., *tbo*-MOFs,[14,15] *rht*-MOFs,[16−19] *soc*-MOFs,[20] *gea*-MOFs,[21] and *eea*-MOFs.[22] Evidently, it is a quite challenging job to explore and construct new MOFs via reticular synthesis.

Inspired by the investigations on copper(I) iodide (denoted as CuI) in MOFs, part of the Cu^+ ions can be easily converted into Cu^{2+} ions in air condition.[23,24] As we know, Cu^+ and I^- ions are easily able to assemble with N donors to form Cu_2I_2 rhomboid dimers and Cu_4I_4 cubane tetramers,[25−30] while Cu^{2+} ions are more likely to coordinate with the O donors to result in the formation of $Cu_2(CO_2)_4$ paddle-wheel SBUs and $Cu(CO_2)_4$ SBUs. If an appropriate ligand contains both N donors and O donors, which can coordinate with CuI to construct many ternary copper SBUs in MOFs.

In this work, HKUST-1, one of the famous MOFs, is chosen as an MOF model, which always can be applied as a candidate for gas adsorption and selectivity.[31] HKUST-1 is formed by 1,3,5-tricarboxybenzene (H_3BTC) linkers and $Cu_2(CO_2)_4$ paddle-wheel SBUs. From the topologic point of view, H_3BTC linkers and $Cu_2(CO_2)_4$ paddle-wheel SBUs can be regarded as 3-connected and 4-connected nodes, respectively. Hence, we selected pyridine-3,5-dicarboxylic acid (denoted as H_2PDC) as an organic linker to react with CuI to construct MOFs. As shown in Scheme 1, H_2PDC can be applied to replace H_3BTC as a 3-connected node, because H_2PDC has two COOH groups to connect with two $Cu_2(COO)_4$ SBUs as two-connected nodes, and one N atom can link with one Cu_xI_y SBU. In addition, H_2PDC contains N donors and O donors synchronously, which can react with CuI to form multiple copper SBUs as 4-connected nodes. Thus, we consider that the

Scheme 1. Schematic Presentation of This Reticular Synthesis Strategy

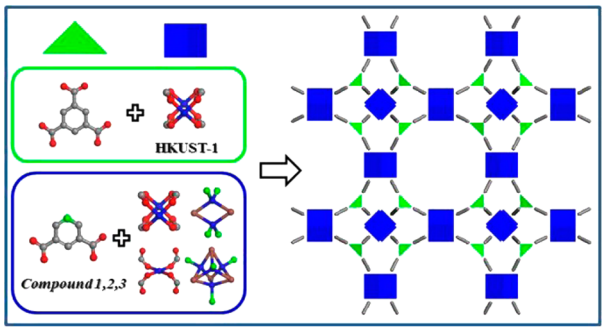

Received: July 4, 2016
Published: August 24, 2016

DOI: 10.1021/acs.inorgchem.6b01592
Inorg. Chem. 2016, 55, 9071−9076

Table 1. Crystal Data and Structure Refinement for Compounds 1, 2, and 3

	compound 1	compound 2	compound 3
empirical formula	$C_{39}H_{39}O_{21}N_9I_3Cu_7$	$C_{40}H_{48}O_{24}N_8I_4Cu_8$	$C_{31}H_{33}O_{16}N_7I_2Cu_5$
formula weight	1798.18	2044.10	1333.21
crystal system	tetragonal	tetragonal	orthorhombic
space group	I_4/mmm	P_4/nmm	$Fmmm$
a (Å)	17.9938(2)	19.1501(17)	21.2731(5)
b (Å)	17.9938(2)	19.1501(17)	25.7339(6)
c (Å)	22.1829(5)	11.1190(12)	27.1818(7)
α (deg)	90.00	90.00	90.00
β (deg)	90.00	90.00	90.00
γ (deg)	90.00	90.00	90.00
V (Å^3)	7182.3(2)	4077.6(8)	14880.4(6)
Z	4	8	8
ρ_{calc} (g cm^{-3})	1.468	1.418	1.128
μ (mm^{-1})	9.490	14.511	8.464
N_{ref}	1923	2138	3744
$F(000)$	3060.0	1624.0	4824.0
R(int)	0.0581	0.0868	0.0438
Goodness-of-fit on F^2	1.045	1.060	1.072
R_1, wR_2 [$I > 2\sigma(I)$]	0.0468, 0.1470	0.037, 0.1069	0.1099, 0.2954
R_1, wR_2 (all data)	0.0478, 0.1480	0.0413, 0.1106	0.1156, 0.3031

ligand can coordinate with CuI to form HKUST-like MOFs based on multiple four-node copper SBUs.

As we expected, a series of porous HKUST-like MOFs were successfully synthesized via this reticular synthesis approach. The as-synthesized samples of compounds **1**, **2**, and **3** as green crystals were successfully prepared by heating ligand H_2PDC with CuI in different conditions, namely, $(Cu_2I_2)[Cu_2PDC_2(H_2O)_2]_2{\cdot}[Cu(MeCN)_4]I{\cdot}DMF$ (compound **1**), $(Cu_4I_4)[Cu_2PDC_2(H_2O)_2]_2{\cdot}4DMF$ (compound **2**), and $(Cu_2I_2)[Cu_3PDC_3(H_2O)_2]{\cdot}2MeCN{\cdot}2DMF$ (compound **3**), (DMF, *N*,*N*-dimethylformamide and MeCN, acetonitrile). Compound **1** is constructed by two SBUs: $Cu_2(CO_2)_4$ paddle-wheel SBUs and Cu_2I_2 dimer SBUs. Compound **2** has $Cu_2(CO_2)_4$ paddle-wheel SBUs and Cu_4I_4 SBUs. Furthermore, compound **3** possesses $Cu_2(CO_2)_4$ paddle-wheel SBUs, Cu_2I_2 dimer SBUs, and $Cu(CO_2)_4$ SBUs. These compounds are promising porous materials for CO_2 capture and separation, because they all display commendable adsorption of CO_2 and high selectivity for CO_2 over CH_4 and N_2. It is worthy to note that compound **1** exhibits the highest Brunauer–Emmett–Teller (BET) surface area (ca. 901 m^2 g^{-1}) among the MOF materials based on Cu_xI_y SBUs.[32−36] In addition, compound **3** is the first case that three copper SBUs coexist in MOFs.

EXPERIMENTAL SECTION

Materials and Methods. Pyridine-3,5-dicarboxylic acid (H_2PDC) and copper(I) iodide (CuI) were purchased from Sigma-Aldrich. 1,4-Diazabicyclo[2.2.2]octane (dabco) and tetrabutylammonium bromide (TATBr) were achieved from Aladdin Reagent. All the chemical solvents were used as received without further purification. Powder X-ray diffraction (PXRD) patterns were obtained on a Scintag X1 diffractometer with Cu–Kα (λ = 1.5418 Å) at 50 kV, 200 mA, in the range of 5–40° (2θ). Thermogravimetric analyses (TGA) for all measurements were carried on a PerkinElmer TGA thermogravimetric analyzer under nitrogen flow at a heating rate of 10 °C/min in the range of 30–800 °C. Elemental analyses (C, H, and N) were acquired from a PerkinElmer 240 analyzer. Fourier transform infrared spectra (FT-IR) were performed on a Nicolet Impact 410 FT-IR spectrometer in the 4000–400 cm^{-1} range using KBr pellets. All gas sorption measurements were acquired on the surface area analyzer ASAP 2020.

Synthesis of Compound 1. A mixture of H_2PDC (15 mg, 0.09 mmol), dabco (10 mg, 0.09 mmol), and DMF (3 mL) was put into a 20 mL vessel. Another mixture of CuI (30 mg, 0.16 mmol) and MeCN (2 mL) was added into a 20 mL vessel. They were mixed together, and aqueous HNO_3 solution (0.15 mL, 2.0 M) was added, which was sealed into a 20 mL capped vessel. It was heated at 85 °C for 1 day and then allowed to cool to room temperature. The green crystals were obtained with the yield of 74% (based on the ligand). Element analysis (%) Calc. for $C_{39}H_{39}O_{21}N_9I_3Cu_7$: C, 26.03; H, 2.17; N, 7.00; Found: C, 26.39; H, 2.27; N, 7.06. Selected FT-IR data (KBr pellet, cm^{-1}): 3312 (br), 1641 (s), 1436 (s), 1376 (s), 1288 (s), 1122 (s), 1031 (s), 828 (s), 765 (s), 737 (s), 662 (s), 495 (s) (Figure S1).

Synthesis of Compound 2. A mixture of H_2PDC (5 mg, 0.03 mmol), CuI (16 mg, 0.084 mmol), tetrabutylammonium bromide (TATBr, 20 mg, 0.062 mmol), DMF (1 mL), and HNO_3 (0.3 mL, 2.5 M in DMF) was sealed into a 20 mL capped vessel. The as-synthesized green block crystals can be obtained after 1 day at 85 °C. The yield is about 79% (based on the ligand). Element analysis (%) Calc. for $C_{40}H_{48}O_{24}N_8I_4Cu_8$: C, 23.48; H, 2.35; N, 5.48; Found: C, 23.29; H, 2.41; N, 5.41. Selected FT-IR data (KBr pellet, cm^{-1}): 3312 (br), 1641 (s), 1436 (s), 1376 (s), 1288 (s), 1153 (s), 1102 (s), 1031 (s), 828 (s), 765 (s), 737 (s), 663 (s), 495 (s).

Synthesis of Compound 3. A mixture of H_2PDC (15 mg, 0.09 mmol), dabco (10 mg, 0.09 mmol), and DMF (3 mL) was put into a 20 mL vessel. The other mixture of CuI (30 mg, 0.16 mmol), TATBr (50 mg, 0.155 mmol), and MeCN (2 mL) was added into another 20 mL vessel. They were mixed together and aqueous HNO_3 solution (0.13 mL, 2.0 M) was added to obtain a clear reaction solution, which was sealed into a 20 mL capped vessel. It was heated at 85 °C for 4 days to achieve the green crystals with the yield of 43% (based on the ligand). Element analysis (%) Calc. for $C_{31}H_{33}O_{16}N_7I_2Cu_5$: C, 27.91; H, 2.48; N, 7.35; Found: C, 27.98; H, 2.56; N, 7.49. Selected FT-IR data (KBr pellet, cm^{-1}): 3312 (br), 3045 (br), 1641 (s), 1449 (s), 1361 (s), 1284 (s), 1098 (s), 824 (s), 765 (s), 728 (s), 676 (s), 592 (s), 495 (s), 464 (s).

Single-Crystal X-ray Crystallography. X-ray diffraction data for compound **1**, compound **2**, and compound **3** were collected on a Bruker SMART APEX II CCD with Cu–Kα radiation (λ = 1.5418 Å) at 100 K. The SADABS program was applied to correct the diffracted beam absorption effects.[37] Their structures can be successfully obtained by a combination of direct methods and refined by full-matrix least-squares against F^2 values using the SHELXTL program.[38] All non-hydrogen atoms were found successfully from Fourier maps, which were further refined by anisotropic thermal parameters. Due to

DOI: 10.1021/acs.inorgchem.6b01592
Inorg. Chem. 2016, 55, 9071−9076

some disordered solvent or coordinated molecules in compound **1**, compound **2**, and compound **3**, their diffraction contributions were removed via the PLATON/SQUEEZE route.[39,40] These molecules can be determined from the TGA data and elemental analyses (C, H, and N). Crystallographic data collection and refinement parameters for these compounds are found in Table 1 and deposited with the Cambridge Crystallographic Data Center (CCDC: 1482037, 1482038, and 1482039). The selected bond distances and angles are listed in Table S2.

RESULTS AND DISCUSSION

Structure Description. Single-crystal X-ray structure studies demonstrate that compound **1**, compound **2**, and compound **3** crystallize in tetragonal space group *I*4/*mmm*, tetragonal space group *P*4/*nmm*, and orthorhombic space group *Fmmm*, respectively. The asymmetrical units are shown in Figures S2–S4. Because the H_2PDC ligand contains N donors and O donors synchronously, the N donors easily coordinate with Cu^+ and I^- ions to form Cu_xI_y clusters, while the O donors easily coordinate with Cu^{2+} ions to result in the formation of $Cu_x(CO_2)_y$ clusters. As shown in Figure 1a,

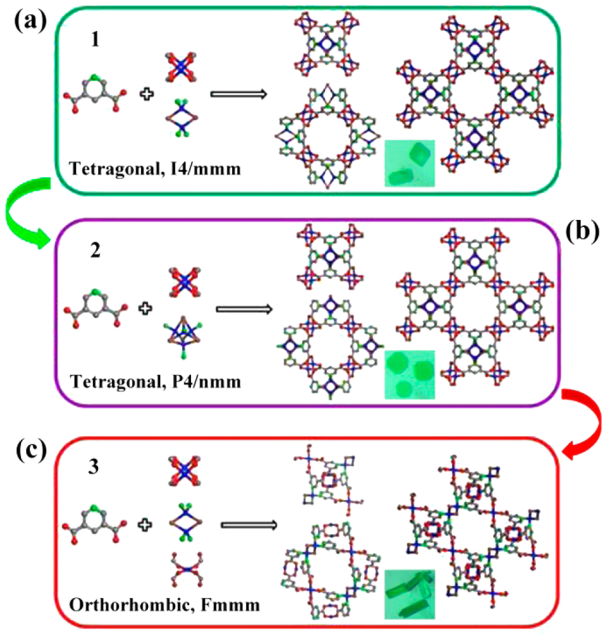

Figure 1. Description of the ligand H_2PDC, the SBUs, and the 3 D structures in compound **1** (a), compound **2** (b), and compound **3** (c) with the optical photos (Cu: blue; N: green; C: gray; O: red; I: brown).

compound **1** is constructed by two SBUs: $Cu_2(CO_2)_4$ paddle-wheel SBUs and Cu_2I_2 dimer SBUs. Compound **2** has $Cu_2(CO_2)_4$ paddle-wheel SBUs and Cu_4I_4 SBUs (Figure 1b). Furthermore, compound **3** possesses $Cu_2(CO_2)_4$ paddle-wheel SBUs, Cu_2I_2 dimer SBUs, and $Cu(CO_2)_4$ SBUs (Figure 1c), which may be attributed to TBABr and solvent effects. The H_2PDC ligand can be regarded as a 3-connected linker, and all SBUs can be simplified as four-connected nodes, which can be further assembled to generate three-dimensional (3 D) porous architectures like the structure of HKUST-1.

PXRD and Thermal Analysis. The powder X-ray diffraction (PXRD) patterns of compound **1**, compound **2**, and compound **3** were carried out at room temperature. As shown in Figures S5–S7, the characteristic peaks of these as-synthesized samples closely matched those of their simulated patterns, which demonstrated the phase purity of these bulk crystalline materials. From the TGA analyses (Figure S8), compound **1** exhibited a slow weight loss of 27.13% before 220 °C (calculated 27.81%). The TGA curve showed a weight loss of 17.27% before 220 °C for compound **2** (calculated 17.81%). For compound **3**, it is found that there was a weight loss of 19.27% before 240 °C (calculated 19.80%). The weight losses were mainly attributable to the loss of guest and coordinated molecules. Then, the frameworks decomposed gradually with the increase of temperature.

Gas Sorption Properties. Considering the existence of permanent porosity, gas sorption for these desolvated **1**, **2**, and **3** was performed. The fresh compound **1** was soaked in dichloromethane for 3 days and activated about 10 h under room temperature. The synthesized samples of compound **2** were exchanged with methanol for 3 days, then desolvated at 100 °C for 12 h under vacuum. The synthesized samples of compound **3** were exchanged with methanol and activated using a supercritical CO_2 drying method.[41] As shown in Figures S6–S8, the PXRD patterns of these activated samples indicated that the original skeletons were still retained after activation. As shown in Figure 2, the N_2 adsorption isotherms of such

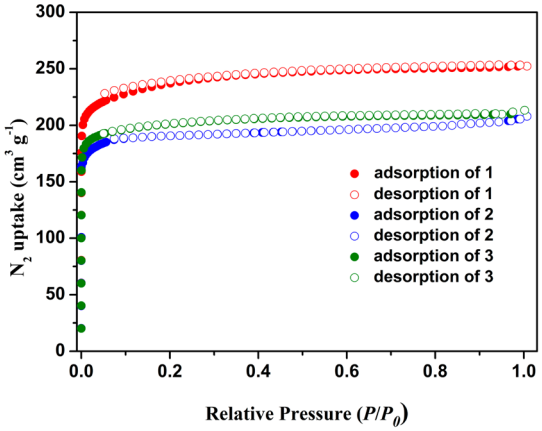

Figure 2. N_2 sorption isotherms of activated compound **1** (red), compound **2** (blue), and compound **3** (green) at 77 K (solid symbols: adsorption, and open symbols: desorption).

activated samples at 77 K were increased to 228, 188, 197 cm^3 g^{-1} by sharp gas uptakes at the low-pressure region (P/P_0 < 0.1), respectively. The results demonstrated that these porous materials belong to microporous materials with completely reversible type-I adsorption behavior characteristics. The BET surface area and Langmuir surface area were calculated to be about 901 and 1025 m^2 g^{-1} for compound **1**, 745 and 835 m^2 g^{-1} for compound **2**, and 775 and 871 m^2 g^{-1} for compound **3**, respectively. Especially, compound **1** exhibits the highest BET surface area among all the MOF materials based on Cu_xI_y SBUs, not only because $Cu_2(CO_2)_4$ paddle-wheel SBUs and Cu_2I_2 dimer SBUs are lighter than the other Cu_xI_y SBUs but also because the HKUST-like structures always have high BET surface areas in MOFs.

Some other small gases (CO_2, N_2, and CH_4) were further measured for the sorption behaviors of activated samples. In addition, the adsorption enthalpy (Q_{st}) can be calculated according to the adsorption isotherms at 273 and 298 K using the *virial* method.[42] For the desolvated compound **1**, the CO_2 adsorption was observed to be 115.26 cm^3 g^{-1} (5.15 mmol g^{-1})

DOI: 10.1021/acs.inorgchem.6b01592
Inorg. Chem. 2016, 55, 9071–9076

and 84.01 $cm^3\ g^{-1}$ (3.75 mmol g^{-1}) at 273 and 298 K under 1 atm (Figure 3a). The Q_{st} of CO_2 is 26.0 kJ mol^{-1} at zero

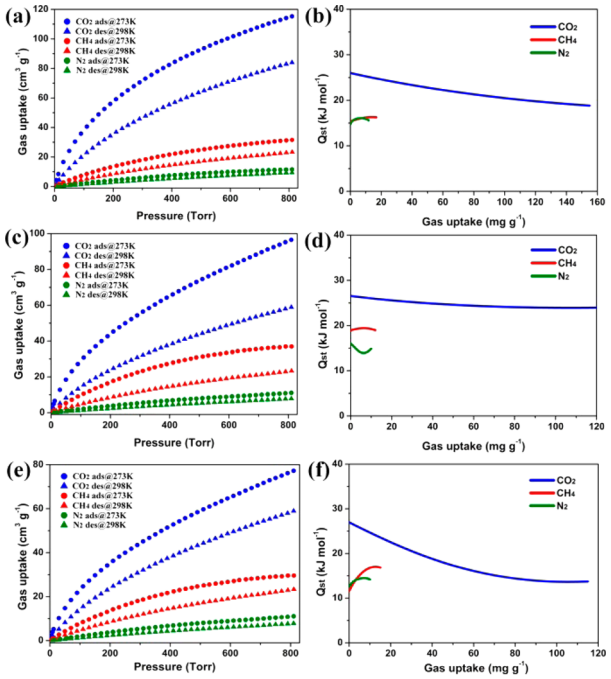

Figure 3. Gas adsorption isotherms of CO_2, CH_4, and N_2 at 273 and 298 K and the Q_{st} of these gases of compound **1** (a, b), compound **2** (c, d), and compound **3** (e, f).

loading (Figure 3b and Figure S9). In addition, the sorption isotherms of N_2 and CH_4 were measured at 273 and 298 K under 1 atm (Figure 3a). The maximum adsorptions for N_2 are 11.60 $cm^3\ g^{-1}$ (0.52 mmol g^{-1}) and 9.45 $cm^3\ g^{-1}$ (0.42 mmol g^{-1}), and CH_4 are 31.56 $cm^3\ g^{-1}$ (1.41 mmol g^{-1}) and 23.29 $cm^3\ g^{-1}$ (1.04 mmol g^{-1}), respectively. At zero loading, the Q_{st} of N_2 and CH_4 are 14.77 and 15.43 kJ mol^{-1}, respectively (Figure 3b, Figures S10 and S11). For the desolvated compound **2**, the CO_2 adsorption was about 91.01 $cm^3\ g^{-1}$ (4.06 mmol g^{-1}) and 62.31 $cm^3\ g^{-1}$ (2.78 mmol g^{-1}) at 273 and 298 K under 1 atm (Figure 3c). The Q_{st} of CO_2 is 26.56 kJ mol^{-1} at zero loading (Figure 3d and Figure S12). The sorption isotherms of N_2 and CH_4 were both measured at 273 and 298 K under 1 atm (Figure 3c). The maximum adsorption uptakes for N_2 are 12.29 $cm^3\ g^{-1}$ (0.55 mmol g^{-1}) and 7.65 $cm^3\ g^{-1}$ (0.34 mmol g^{-1}), and CH_4 are 26.01 $cm^3\ g^{-1}$ (1.16 mmol g^{-1}) and 17.03 $cm^3\ g^{-1}$ (0.76 mmol g^{-1}), respectively. At zero loading, the Q_{st} of N_2 and CH_4 are 15.96 and 18.93 kJ mol^{-1}, respectively (Figure 3d, Figures S13 and S14). For the desolvated compound **3**, the CO_2 adsorption uptake was about 77.23 $cm^3\ g^{-1}$ (3.45 mmol g^{-1}) and 58.94 $cm^3\ g^{-1}$ (2.63 mmol g^{-1}) at 273 and 298 K under 1 atm (Figure 3e). The Q_{st} of CO_2 is 26.98 kJ mol^{-1} at zero loading (Figure 3e and Figure S15). In addition, the maximum adsorption amounts for N_2 are 11.08 $cm^3\ g^{-1}$ (0.49 mmol g^{-1}) and 7.82 $cm^3\ g^{-1}$ (0.35 mmol g^{-1}), and CH_4 are 29.57 $cm^3\ g^{-1}$ (1.32 mmol g^{-1}) and 22.65 $cm^3\ g^{-1}$ (1.01 mmol g^{-1}), respectively. At zero loading, the Q_{st} of N_2 and CH_4 are about 12.50 and 11.57 kJ mol^{-1}, respectively (Figure 3e, Figures S16 and S17). Particularly, the Q_{st} values of compound **1**, compound **2**, and compound **3** for CO_2 are higher than those of most "benchmark MOFs", such as CuBTTri (21 kJ mol^{-1}),[43] MOF-5 (17 kJ mol^{-1}),[44] UMCM-1 (12 kJ mol^{-1}),[45] and NOTT-140 (25 kJ mol^{-1}),[46] and are further comparable to that of MIL-53(Cr) (32 kJ mol^{-1}),[47] HKUST-1 (hydrated) (30 kJ mol^{-1}),[48] MAF-2 (27 kJ mol^{-1}),[49] JUC-132 (30 kJ mol^{-1}),[50] and JLU-Liu22 (30 kJ mol^{-1}).[51] It is mainly due to the strong interactions between CO_2 molecules and exposed Cu sites in the host frameworks.

Theoretical different gas mixtures of CO_2/N_2 and CO_2/CH_4 are calculated by the IAST model to evaluate the practical separation ability for CO_2. The IAST model is always applied as a conventional route to predict binary mixture separating capacity from experimental single-component adsorption isotherms. The adsorption isotherms were successfully fitted to predict the multicomponent selectivity using the dual-site Langmuir–Frendlich equation (Figure 4a,c,e). The predicated

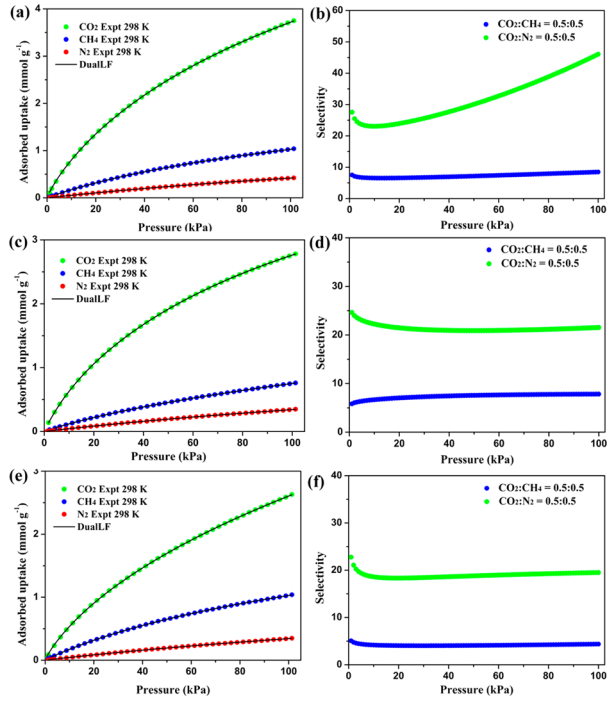

Figure 4. Gas sorption isotherms of CO_2, CH_4, and N_2 along with the dual-site Langmuir–Freundlich (DSLF) fits (a, c, e); gas mixture adsorption selectivities are predicted by IAST at 298 K under 101 kPa (b, d, f).

results were calculated from a function of pressure at a general feed composition of landfill gas (50/50, m/m) at 298 K under 101 kPa (Figure 4b,d,f). At 298 K and 101 kPa, the selectivity values for CO_2/CH_4 and CO_2/N_2 are 9 and 46 for compound **1**, 8 and 22 for compound **2**, and 4 and 20 for compound **3**, respectively. The selectivity values are clearly higher than those of many reported MOFs under the similar conditions.[52−54] These results suggest that these porous HKUST-like MOFs are good candidates for capture and separate CO_2, because the higher quadrupole moment of CO_2 (43.0×10^{-27} $esu^{-1}\ cm^{-1}$) triggers stronger interaction with exposed Cu sites of the host framework.[55]

CONCLUSION

In summary, we successfully designed and synthesized a series of porous HKUST-like MOFs via the reticular synthesis approach. They are constructed by H_2PDC and multiple copper SBUs, including $Cu_2(CO_2)_4$ paddle-wheel SBUs,

DOI: 10.1021/acs.inorgchem.6b01592
Inorg. Chem. 2016, 55, 9071−9076

$Cu(CO_2)_4$ SBUs, Cu_2I_2 dimer SBUs, and Cu_4I_4 SBUs. These compounds can be used as porous materials for CO_2 capture and separation, because they all display commendable adsorption of CO_2 and high selectivity for CO_2 over CH_4 and N_2. It is worthy to note that compound **1** exhibits the highest BET surface area (ca. 901 $m^2\ g^{-1}$) among the MOF materials based on Cu_xI_y SBUs. In addition, compound **3** is the first case that three copper SBUs coexist in MOFs. Further work about employing this strategy is ongoing in our laboratories.

■ ASSOCIATED CONTENT

Supporting Information

The Supporting Information is available free of charge on the ACS Publications website at DOI: 10.1021/acs.inorgchem.6b01592.

PXRD, TGA, and FT-IR (PDF)
Crystallographic data (CIF)
Crystallographic data (CIF)
Crystallographic data (CIF)

■ AUTHOR INFORMATION

Corresponding Authors

*E-mail: sqma@usf.edu (S.M.).
*E-mail: zhugs@jlu.edu.cn. Fax: +86-431-85168331. Tel: +86-0431-85168887 (G.Z.).

Author Contributions

The manuscript was written through contributions of all authors. All authors have given approval to the final version of the manuscript.

Notes

The authors declare no competing financial interest.

■ ACKNOWLEDGMENTS

We are grateful for the financial support of the National Basic Research Program of China (973 Program, grant nos. 2012CB821700 and 2014CB931804), the Major International (Regional) Joint Research project of NSFC (grant no. 21120102034), NSFC Project (grant no. 21531003), NSF (DMR-1352065), and USF.

■ REFERENCES

(1) Jiang, J.; Yaghi, O. M. *Chem. Rev.* **2015**, *115*, 6966−6997.
(2) Zhou, H.-C.; Kitagawa, S. *Chem. Soc. Rev.* **2014**, *43*, 5415−5418.
(3) Zhou, H.-C.; Long, J. R.; Yaghi, O. M. *Chem. Rev.* **2012**, *112*, 673−674.
(4) Li, B.; Chrzanowski, M.; Zhang, Y.; Ma, S. *Coord. Chem. Rev.* **2016**, *307*, 106−129.
(5) He, H.; Song, Y.; Sun, F.; Zhao, N.; Zhu, G. *Cryst. Growth Des.* **2015**, *15*, 2033−2038.
(6) Liu, H.; Xi, F.-G.; Sun, W.; Yang, N.-N.; Gao, E.-Q. *Inorg. Chem.* **2016**, *55*, 5753−5755.
(7) He, H.; Song, Y.; Sun, F.; Bian, Z.; Gao, L.; Zhu, G. *J. Mater. Chem. A* **2015**, *3*, 16598−16603.
(8) Lin, X.-M.; Niu, J.-L.; Wen, P.-X.; Pang, Y.; Hu, L.; Cai, Y.-P. *Cryst. Growth Des.* **2016**, *16*, 4705−4710.
(9) Fu, H.-R.; Zhang, J. *Inorg. Chem.* **2016**, *55*, 3928−3932.
(10) He, H.; Sun, F.; Borjigin, T.; Zhao, N.; Zhu, G. *Dalton Trans.* **2014**, *43*, 3716−3721.
(11) Liu, L.; Wang, S.-M.; Han, Z.-B.; Ding, M.; Yuan, D.-Q.; Jiang, H.-L. *Inorg. Chem.* **2016**, *55*, 3558−3565.
(12) Horcajada, P.; Chalati, T.; Serre, B.; Gillet, B.; Sebrie, C.; Eubank, T. B. J. F.; Heurtaux, A.; Clayette, P.; Kreuz, C.; Chang, J.-S.; Hwang, Y. K.; Marsaud, V.; Bories, P.-N.; Cynober, L.; Gil, S.; Ferey, G.; Couvrenur, P.; Gref, R.; Baati, T. *Nat. Mater.* **2010**, *9*, 172−178.
(13) He, H.; Sun, F.; Jia, J.; Bian, Z.; Zhao, N.; Qiu, X.; Gao, L.; Zhu, G. *Cryst. Growth Des.* **2014**, *14*, 4258−4261.
(14) Spanopoulos, I.; Tsangarakis, C.; Klontzas, E.; Tylianakis, E.; Froudakis, G.; Adil, K.; Belmabkhout, Y.; Eddaoudi, M.; Trikalitis, P. N. *J. Am. Chem. Soc.* **2016**, *138*, 1568−1574.
(15) Eubank, J. F.; Mouttaki, H.; Cairns, A. J.; Belmabkhout, Y.; Wojtas, L.; Luebke, R.; Alkordi, M.; Eddaoudi, M. *J. Am. Chem. Soc.* **2011**, *133*, 14204−14207.
(16) Eubank, J. F.; Nouar, F.; Luebke, R.; Cairns, A. L.; Wojtas, L.; Alkordi, M.; Bousquet, T.; Hight, M. R.; Eckert, J.; Embs, J. P.; Georgiev, P. A.; Eddaoudi, M. *Angew. Chem., Int. Ed.* **2012**, *51*, 10099−10103.
(17) Luebke, R.; Eubank, J. F.; Cairns, A. J.; Belmabkhout, Y.; Wojtas, L.; Eddaoudi, M. *Chem. Commun.* **2012**, *48*, 1455−1457.
(18) Liu, K.; Li, B.; Li, Y.; Li, X.; Yang, F.; Zeng, G.; Peng, Y.; Zhang, Z.; Li, G.; Shi, Z.; Feng, S.; Song, D. *Chem. Commun.* **2014**, *50*, 5031−5033.
(19) Zheng, B.; Bai, J.; Duan, J.; Wojtas, L.; Zaworotko, M. J. *J. Am. Chem. Soc.* **2011**, *133*, 748−751.
(20) Alezi, D.; Belmabkhout, Y.; Suyetin, M.; Bhatt, P. M.; Weselinski, L. J.; Solovyeva, V.; Adil, K.; Spanopoulos, I.; Trikalitis, P. N.; Emwas, A.; Eddaoudi, M. *J. Am. Chem. Soc.* **2015**, *137*, 13308−13318.
(21) Guillerm, V.; Weseliński, L. J.; Belmabkhout, Y.; Cairns, A. J.; D'Elia, V.; Wojtas, L.; Adil, K.; Eddaoudi, M. *Nat. Chem.* **2014**, *6*, 673−680.
(22) Chen, Z.; Adil, K.; Weseliński, L. J.; Belmabkhout, Y.; Eddaoudi, M. *J. Mater. Chem. A* **2015**, *3*, 6276−6281.
(23) Zhang, J.-P.; Zhang, Y.-B.; Lin, J.-B.; Chen, X.-M. *Chem. Rev.* **2012**, *112*, 1001−1033.
(24) Yu, Q.; Zhu, L.-G.; Bian, H.-D.; Deng, J.-H.; Bao, X.-G.; Liang, H. *Inorg. Chem. Commun.* **2007**, *10*, 437−439.
(25) Abdulhalim, R. G.; Shkurenko, A.; Alkordi, M. H.; Eddaoudi, M. *Cryst. Growth Des.* **2016**, *16*, 722−727.
(26) Kitagawa, H.; Ohtsu, H.; Kawano, M. *Angew. Chem., Int. Ed.* **2013**, *52*, 12395−12399.
(27) Wang, J.; Luo, J.; Luo, X.; Zhao, J.; Li, S.-S.; Li, G.; Huo, Q.; Liu, Y. *Cryst. Growth Des.* **2015**, *15*, 915−920.
(28) Zhao, C.-W.; Ma, J.-P.; Liu, Q.-K.; Wang, X.-R.; Liu, Y.; Yang, J.; Yang, J.-S.; Dong, Y.-B. *Chem. Commun.* **2016**, *52*, 5238−5241.
(29) Fu, Z.; Lin, J.; Wang, L.; Li, C.; Yan, W.; Wu, T. *Cryst. Growth Des.* **2016**, *16*, 2322−2327.
(30) Luo, X.; Sun, L.; Zhao, J.; Li, D.-S.; Wang, D.; Li, G.; Huo, Q.; Liu, Y. *Cryst. Growth Des.* **2015**, *15*, 4901−4907.
(31) Chui, S. S.-Y.; Lo, S. M.-F.; Charmant, J. P. H.; Orpen, A. G.; Williams, I. D. *Science* **1999**, *283*, 1148−1150.
(32) Kang, Y.; Wang, F.; Zhang, J.; Bu, X. *J. Am. Chem. Soc.* **2012**, *134*, 17881−17884.
(33) Qian, J.; Jiang, F.; Su, K.; Pan, J.; Liang, L.; Mao, F.; Hong, M. *Cryst. Growth Des.* **2015**, *15*, 1440−1445.
(34) Qian, J.; Jiang, F.; Su, K.; Pan, J.; Xue, Z.; Liang, L.; Bag, P. P.; Hong, M. *Chem. Commun.* **2014**, *50*, 15224−15227.
(35) Luo, X.; Cao, Y.; Wang, T.; Li, G.; Li, J.; Yang, Y.; Xu, Z.; Zhang, J.; Huo, Q.; Liu, Y.; Eddaoudi, M. *J. Am. Chem. Soc.* **2016**, *138*, 786−789.
(36) Yang, T.; Cui, H.; Zhang, C.; Zhang, L.; Su, C.-Y. *Inorg. Chem.* **2013**, *52*, 9053−9059.
(37) Sheldrick, G. M. *SADABS: Program for Empirical Absorption Correction for Area Detector Data*; University of Göttingen: Göttingen, Germany, 1996.
(38) Sheldrick, G. M. *SHELXTL Version 5.1 Software Reference Manual*; Bruker AXS, Inc.: Madison, WI, 1997.
(39) Spek, A. L. *J. Appl. Crystallogr.* **2003**, *36*, 7.
(40) Spek, A. L. *PLATON: A Multipurpose Crystallographic Tool*; Utrecht University: Utrecht, The Netherlands, 2001.
(41) Nelson, A. P.; Farha, O. K.; Mulfort, K. L.; Hupp, J. T. *J. Am. Chem. Soc.* **2009**, *131*, 458−460.

DOI: 10.1021/acs.inorgchem.6b01592
Inorg. Chem. 2016, 55, 9071−9076

(42) Czepirski, L.; Jagiello, J. *Chem. Eng. Sci.* **1989**, *44*, 797−801.
(43) Demessence, A. D.; D'Alessandro, M.; Foo, M. L.; Long, J. R. *J. Am. Chem. Soc.* **2009**, *131*, 8784−8786.
(44) Choi, J.-S.; Son, W.-J.; Kim, J.; Ahn, W.-S. *Microporous Mesoporous Mater.* **2008**, *116*, 727−731.
(45) Mu, B.; Schoenecker, P. M.; Walton, K. S. *J. Phys. Chem. C* **2010**, *114*, 6464−6471.
(46) Tan, C.; Yang, S.; Champness, N. R.; Lin, X.; Blake, A. J.; Lewis, W.; Schröder, M. *Chem. Commun.* **2011**, *47*, 4487−4489.
(47) Bourrelly, S.; Llewellyn, P. L.; Serre, C.; Millange, F.; Loiseau, T.; Férey, G. *J. Am. Chem. Soc.* **2005**, *127*, 13519−13521.
(48) Liang, Z.; Marshall, M.; Chaffee, A. L. *Energy Procedia* **2009**, *1*, 1265−1271.
(49) Zhang, J.-P.; Chen, X.-M. *J. Am. Chem. Soc.* **2009**, *131*, 5516−5521.
(50) He, H.; Song, Y.; Zhang, C.; Sun, F.; Yuan, R.; Bian, Z.; Gao, L.; Zhu, G. *Chem. Commun.* **2015**, *51*, 9463−9466.
(51) Wang, D.; Liu, B.; Yao, S.; Wang, T.; Li, G.; Huo, Q.; Liu, Y. *Chem. Commun.* **2015**, *51*, 15287−15289.
(52) Li, R.-J.; Li, M.; Zhou, X.-P.; Li, D.; O'Keeffe, M. *Chem. Commun.* **2014**, *50*, 4047−4049.
(53) Sumida, K.; Rogow, D. L.; Mason, J. A.; McDonald, T. M.; Bloch, E. D.; Herm, Z. R.; Bae, T.-H.; Long, J. R. *Chem. Rev.* **2012**, *112*, 724−781.
(54) Zheng, B.; Lin, X.; Wang, Z.; Yun, R.; Fan, Y.; Ding, M.; Hu, X.; Yi, P. *CrystEngComm* **2014**, *16*, 9586−9589.
(55) Liu, B.; Smit, B. *Langmuir* **2009**, *25*, 5918−5926.

DOI: 10.1021/acs.inorgchem.6b01592
Inorg. Chem. 2016, 55, 9071−9076